Skeletal Radiol (2016) 45:1031–1043
DOI 10.1007/s00256-016-2390-y

REVIEW ARTICLE

Understanding carpal instability: a radiographic perspective

Kimia Khalatbari Kani[1] · **Hyojeong Mulcahy**[2] · **Felix S. Chew**[2]

Received: 6 February 2016 / Revised: 26 March 2016 / Accepted: 6 April 2016 / Published online: 16 April 2016

Abstract The wrist is disposed to a variety of instability patterns owing to its complex anatomical and biomechanical properties. Various classification schemes have been proposed to describe the different patterns of carpal instability, of which the Mayo classification is the most commonly used. Understanding the concepts and pertinent terminology of this classification scheme is important for the correct interpretation of images and optimal communication with referring physicians. Standard wrist radiographs are the first line of imaging in carpal instability. Additional information may be obtained with the use of stress radiographs and other imaging modalities.

Keywords Carpal instability · Mayo classification · Scapholunate instability · Lunotriquetral instability · Axial instability · Adaptive carpus

Introduction

The wrist is the link between the forearm and the hand. The wrist's complex anatomical and biomechanical properties permit the versatile positioning of the hand and the transmission of force to or from the body. Carpal instability can be described as abnormal kinematics where the wrist is unable to bear physiological loads [1]. However, a consistent description of carpal instability as a clinical entity is difficult to find. Different classification schemes have been used to organize the variety of instability patterns observed [2, 3], of which the Mayo classification is most commonly used. In this classification scheme carpal instability is divided into four major patterns:

1. "Carpal instability dissociative" occurs among the proximal or distal carpal rows of bones.
2. "Carpal instability nondissociative" takes place at the radiocarpal and/or midcarpal joint levels.
3. "Carpal instability complex" is a combination of the above two patterns.
4. "Adaptive carpus" refers to instability secondary to morphological abnormalities in the distal radius and/or distal ulna.

Standard wrist radiographs are the first line of imaging in suspected carpal instability. Supplemental (including stress) radiographs and other imaging modalities (such as fluoroscopy with dynamic motion examination, arthrography, MR imaging [MRI]/MR arthrography, CT, traction views obtained with use of anesthesia, and ultrasound) may be necessary for fuller elucidation of carpal abnormalities.

This article reviews the anatomy of the carpus as it pertains to carpal instability, clarifies the commonly used terminology and classification schemes for carpal instability, and describes an analytical approach to the interpretation of wrist radiographs in various forms of carpal instability.

Osseous anatomy

The osseous framework of the carpus includes the radius and ulna, the proximal and distal rows of carpal bones, and the metacarpal bases. From radial to ulnar, the scaphoid, lunate, triquetrum, and pisiform make up the proximal carpal row,

✉ Kimia Khalatbari Kani
khalatbarik@live.com

[1] Advanced Imaging Center, Palmdale, CA, USA

[2] University of WA, Seattle, WA, USA

while the distal carpal row is formed by the trapezium, trapezoid, capitate, and hamate. The complex motions of the wrist occur through three joints: radiocarpal, midcarpal, and carpometacarpal [3].

Except for the pisiform, the bones in each of the proximal and distal carpal rows move in the same primary direction during wrist motion. The pisiform is a sesamoid bone that is ensheathed in the flexor carpi ulnaris tendon and does not participate in the functions of the remaining carpal bones. Aside from the pisiform, there are no tendinous attachments to the carpal bones [3, 4]. Therefore, the scaphoid, lunate, and triquetrum can be considered an "intercalated segment" [5]. Their motion depends primarily on mechanical forces from their proximal and distal articulations, and is checked by an intricate network of carpal ligaments [6, 7].

Ligamentous anatomy

The carpal ligaments can be divided into two broad groups: intrinsic ligaments course between carpal bones, whereas extrinsic ligaments attach the carpal bones to either the radius or the ulna [3]. The intrinsic scapholunate (SL) and lunotriquetral ligaments are considered the primary stabilizers of the proximal carpal row. Both of these ligaments are "U"-shaped (Fig. 1), spanning the dorsal, proximal, and volar aspects of their respective articulations [6]. Microscopically, these ligaments have similar organization, being true ligaments in their dorsal and volar subregions, and membranous in their proximal subregion [8]. The dorsal subregion is the thickest and biomechanically strongest portion of the SL ligament (Fig. 1) and the volar component is the thickest portion of the lunotriquetral ligament [6]. When intact, these two ligaments separate the radiocarpal and midcarpal compartments of the wrist.

At the midcarpal level the intrinsic and extrinsic ligaments form two volar and one dorsal "V"-shaped ligamentous complexes (Fig. 2) [3, 9–11]. Several of these ligaments have been identified as important secondary static stabilizers of the SL and lunotriquetral joints [6, 12, 13].

Carpal kinematics

The wrist provides motion in two planes: flexion/extension and radial/ulnar deviation. Flexion/extension is a relatively straightforward motion occurring at the radiocarpal and midcarpal articulations. In contrast, the kinematics of radioulnar deviation is complex and multiangular [3, 10, 14–16]. Absolutely precise motion allows a smooth and continuous transition from radial to ulnar deviation with maintenance of a constant carpal height throughout the range of motion [3, 10].

Routine radiographic views for the analysis of carpal instability

Conventional radiographs are the first line of imaging in suspected carpal instability. Radiographic evaluation of carpal instability should include a minimum of standard posteroanterior (PA) and lateral views of the wrist [17].

The PA projection is obtained with the wrist in neutral position. The shoulder should be abducted 90°, the elbow flexed 90°, and the wrist should be without evidence of radial or ulnar deviation and flexion or extension. On a true neutral PA view, the extensor carpi ulnaris tendon groove is seen in profile, radial to the midpoint of the ulnar styloid process (Fig. 3a) [18, 19].

A lateral radiograph of the wrist may be obtained with the shoulder adducted and the elbow flexed 90°, with the ulnar aspects of the forearm and hand resting on the Bucky table. The forearm is held between pronation and supination, whereas the wrist has a neutral position with regard to radial/ulnar deviation and flexion/extension [20]. On a true neutral lateral view, the palmar cortex of the pisiform projects between the palmar cortices of the distal scaphoid pole and the capitate head (Fig. 3b) [21].

On a standard PA wrist radiograph the radiocarpal, intercarpal (except for the trapeziotrapezoid joint), midcarpal, and most of the carpometacarpal joints are profiled, parallel, and of similar (1–2 mm) width, and the lunate has a trapezoidal morphology (Fig. 3a). Three fairly smooth arcs outline the radiocarpal and midcarpal joints (Fig. 3a) [22]. Arcs I and II outline the proximal and distal articular surfaces of the scaphoid, lunate, and triquetrum respectively. Arc III follows the proximal convex curvature of the capitate and hamate [22]. Disruption of these arcs, or any overlapping of adjacent bones, commonly indicates underlying carpal instability or fracture. However, two normal variants may simulate step-offs of the carpal arcs:

Fig. 1 Schematic illustration of the scapholunate (SL) ligament. The scaphoid is viewed medially, with other carpal bones removed. Observe that the "U"-shaped SL ligament is thickest dorsally

1. Decreased height of the triquetrum relative to the neighboring lunate creates a step-off of the first arc, with maintenance of a smooth second arc [22]
2. An accessory distal articular facet on the lunate for articulation with the hamate (type II lunate) affects the smooth curvature of the second arc [23]

It is important to derive as much information as possible from the PA radiograph, before surveying the other radiographic projections [22].

The central axes of the radius, lunate, scaphoid, and capitate are used for assessment of carpal alignment on lateral radiographs (Fig. 4). A line parallel to the center of the radial shaft is its axis. The axis of the lunate can be constructed either as a line passing through the centers of its proximal and distal articular surfaces, or as a line perpendicular to a tangential line connecting its distal articular poles [7]. The longitudinal axis of the scaphoid passes through the midpoints of its proximal and distal poles [24]. The axis of the capitate courses through the centers of its head and distal articular surface [24].

The angle between the scaphoid and lunate axes is the scapholunate angle (Fig. 4). Normally, the angle ranges between 30 and 60°, and averages 47° [7]. The angle between the capitate and lunate axes is the capitolunate angle (Fig. 4). Only 11 % of normal individuals demonstrate a coaxial relationship (with the axes of the radius, lunate, capitate, and third metacarpal bones forming a straight line) on lateral radiographs [25]. The capitolunate angle measures between 0 and 30° in normal individuals owing to lunate flexion or capitate extension [25].

Supplemental radiographic views for the analysis of carpal instability

Supplemental radiographic projections may be useful when instability is suspected clinically, but the PA and lateral wrist radiographs appear normal. A variety of radiographic views (including stress views) have been described in this regard [7, 10, 26–29]. The clenched fist view is the most frequently used stress radiograph and can be obtained in the PA or anteroposterior positions, with the central beam passing through the center of the capitate head [30]. The forces created with a clenched fist drive the capitate proximally toward the scapholunate joint, resulting in widening of the joint space in wrists with scapholunate ligament instability [30]. A refined modification is the "clenched pencil" view for exact profiling of the scapholunate space [29]. This PA view is performed with the forearms in pronation while both hands grip a pencil, and allows comparison of the two hands on a single radiograph (Fig. 5).

Posteroanterior radiographs of the wrist in radial and ulnar deviation (Fig. 6), along with lateral projections with the wrist in flexion and extension, may be obtained. With radial deviation, the distal carpal row deviates radially, whereas the proximal carpal row moves reciprocally in the ulnar direction, with the major portion of the lunate moving off the distal radial articular surface [22]. There is also unified flexion of the proximal carpal row with radial deviation. The flexed scaphoid appears foreshortened with its distal pole tilting toward the palm. In this position, the distal scaphoid pole may assume a signet-ring appearance as it is seen end-on. In ulnar deviation,

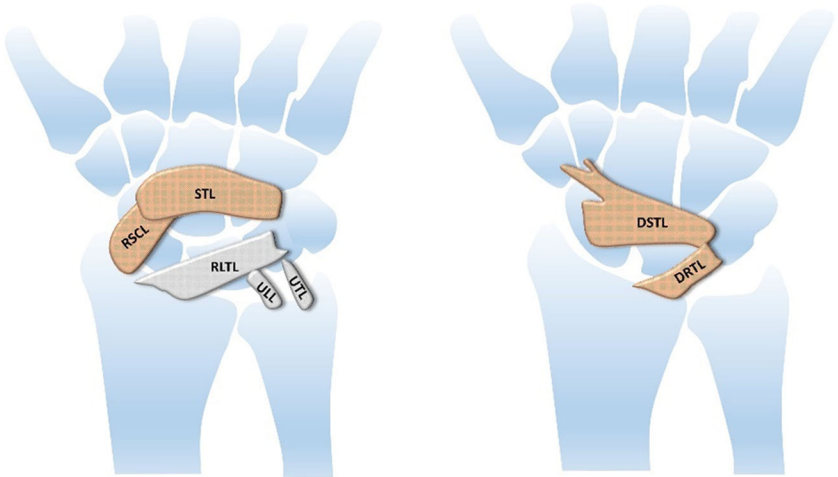

Fig. 2 Simplified schematic illustrations of **a** volar and **b** dorsal carpal ligaments. **a** The volar ligaments are oriented in two reverse "V"-shaped rows (the proximal and distal rows of ligaments are depicted in *gray* and *orange* respectively). *RLTL* radiolunotriquetral ligament (also known as the long radiolunate ligament), *RSCL* radioscaphocapitate ligament, *STL* scaphotriquetral ligament, *ULL* ulnolunate ligament, *UTL* ulnotriquetral ligament. **b** The dorsal carpal ligaments resemble a "V" that is rotated 90°. *DRTL* dorsal radiotriquetral ligament (also known as the dorsal radiocarpal ligament), *DSTL* dorsal scaphotriquetral ligament (also known as the dorsal intercarpal ligament). Various terminologies have been used to describe the volar and dorsal carpal ligaments. Generally, these ligaments are named according to their osseous insertions

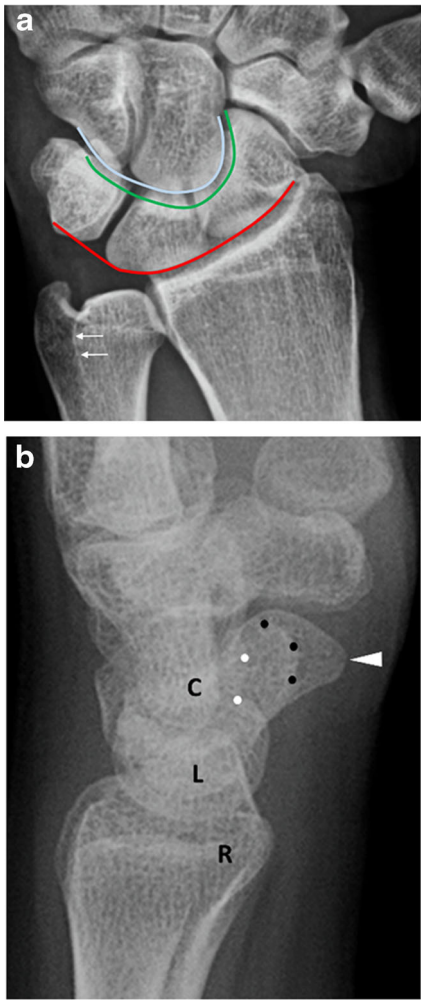

Fig. 3 Standard PA and lateral wrist radiographs of the normal wrist. **a** PA wrist radiograph: the extensor carpi ulnaris groove (*arrows*) is seen in profile radial to the midpoint of the ulnar styloid process. Gilula's arcs I (*red*), II (*green*), and III (*blue*) smoothly outline the proximal and distal carpal rows. Observe the parallel articular surfaces and relatively similar width of the profiled intercarpal, radiocarpal, and midcarpal joints. **b** Lateral wrist radiograph: the palmar cortex of the pisiform (*black dots*) projects between the palmar cortices of the distal scaphoid pole (*arrowhead*) and the capitate head (*white dots*). Observe how the proximal convex articular surface of the lunate (*L*) fits into the distal radius (*R*), whereas its distal concave articular surface closely parallels the capitate head (*C*)

the reverse occurs. The distal carpal row deviates ulnarly, whereas the proximal carpal row moves reciprocally in the radial direction, and there is increased apposition of the lunate with the distal radial articular surface [22]. There is also unified extension of the proximal carpal row, with the extended scaphoid assuming an elongated appearance [22]. The distances between carpal bones are equal and unchanged by radial and ulnar deviation. A scapholunate interval measuring more than 4 mm is considered abnormal, and an interval measuring 2–4 mm may be abnormal [7]. In diagnostically unclear situations, appropriate comparison radiographs may be obtained of the opposite hand [26].

Further imaging can be performed with fluoroscopy and dynamic motion examination, traction views obtained with the use of anesthesia, arthrography, MRI, CT or ultrasound [10]. CT imaging is particularly useful for the evaluation of fractures or fracture–dislocations. MRI can be performed as an unenhanced examination, or as indirect or direct MR arthrography, and is especially useful for assessment of ligament tears. Arthroscopy is considered the gold standard for evaluation of carpal instability and provides the potential for curative surgery in some cases [3, 26].

Classification of carpal instability

The commonly used Mayo classification divides carpal instability into four major categories [3, 31]:

1. "Carpal instability dissociative" (CID), where there is dissociation of the bones in a single carpal row. The proximal carpal row is most commonly affected (i.e., SL instability; lunotriquetral instability). Distal carpal row dissociation is rare.
2. "Carpal instability nondissociative" includes instability at the radiocarpal and/or midcarpal joints.
3. "Carpal instability complex" is a combination of patterns 1 and 2.
4. "Adaptive carpus" refers to carpal instability secondary to congenital or acquired abnormalities in the distal radius and/or distal ulna.

Dorsal intercalated segmental instability (DISI) and volar intercalated segmental instability (VISI) are patterns of carpal malalignment that have a tendency to occur in several carpal instability categories. It is the position of the lunate in either extension (distal lunate articular surface faces dorsally) or flexion (distal lunate articular surface faces volarly) that defines the dorsal or volar pattern of deformity. The term "translocation" is used to describe the direction of displacement (ulnar, radial, volar or dorsal) at the radiocarpal joint level.

Carpal instability may have various causes, including (but not restricted to) trauma, inflammatory arthritis, or congenital abnormalities. Carpal instability can occur acutely, subacutely, or be a chronic condition [3]. Dynamic versus static forms of carpal instability have been emphasized for SL and lunotriquetral instabilities [6, 8]. Dynamic instability describes a deformity only seen on stress radiographs or fluoroscopy, whereas static instability is already visible on routine wrist radiographs (in this article, routine wrist radiographs refer to standard PA and lateral wrist radiographs).

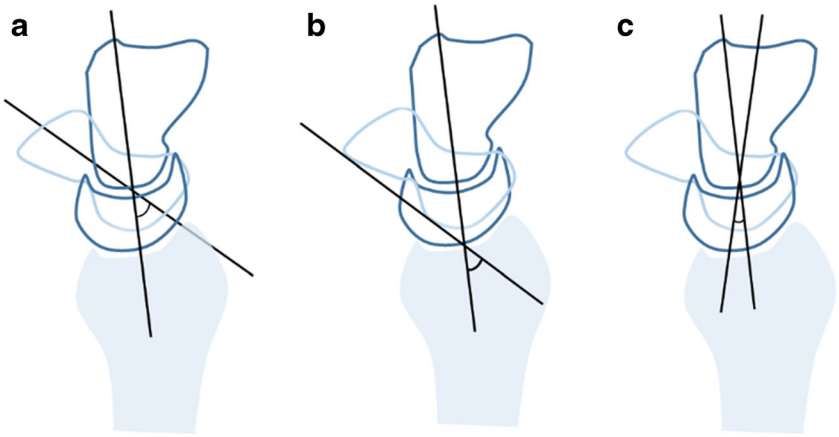

Fig. 4 Scapholunate and capitolunate angles. **a**, **b** The angle between the scaphoid and lunate axes is the scapholunate angle (normal range = 30°–60°). The axis of the lunate can be constructed as a line passing through the centers of its proximal and distal articular surface. The longitudinal axis of the scaphoid passes through the centers of its proximal and distal poles (**a**). The scaphoid axis can also be determined by a line connecting its proximal and distal palmar convexities (**b**). Although this latter line may be off a few degrees, it is usually easier to draw and parallels the true central scaphoid axis closely enough to be reliable. **c** The capitolunate angle (normal = 0°–30°) is formed by the longitudinal capitate and lunate axes. The axis of the capitate courses through the centers of its head and distal articular surface

Proximal row CID: SL instability

Scapholunate instability is the most common form of carpal instability. It may be the result of traumatic injuries to the SL ligament (the most common cause), an unstable scaphoid fracture, rheumatoid arthritis, calcium pyrophosphate deposition disease, and Kienböck's disease [3, 32, 33].

The SL ligament is considered to be the primary stabilizer of the SL joint. Over time, isolated SL ligament injuries, via altered biomechanics and weakening of the secondary stabilizing ligaments of the SL joint, can lead to carpal degeneration and collapse [12, 13, 34]. Therefore, a high index of suspicion is necessary to diagnose SL ligament injuries in the early phases. When clinical examination suggests SL ligament tear and routine radiographs appear normal, stress radiographs, MRI, or arthroscopy may be needed for further evaluation.

The spectrum of SL ligament injuries can be conceptualized in the form of a staging scheme of progressive severity [6, 26, 35]. "Occult" or "pre-dynamic" SL instability results from a partial SL ligament tear [6, 36]. Routine and stress radiographs are normal and fluoroscopy motion studies may be normal or abnormal. Partial SL ligament tears may be assessed with the use of MRI or MR arthrography.

Complete SL ligament disruption with intact secondary stabilizing ligaments may result in "dynamic" SL instability [37–39]. Routine radiographs are usually normal in these symptomatic patients [40], and stress radiographs or fluoroscopy motion studies are necessary for the delineation of abnormalities. Diastasis of the SL interval becomes evident on the clenched fist, clenched pencil, or radial–ulnar deviation views. The clenched pencil view is considered to be the best stress view for demonstrating

Fig. 5 Clenched pencil view in a 32-year-old woman. There is left SL instability with asymmetric widening (8 mm; *arrows*) of the left SL joint

Fig. 6 PA radiographs of the normal wrist in radial and ulnar deviation in a 35-year-old man. **a** With radial deviation the distal carpal row and metacarpal bones move as a single unit in the radial direction (*black arrow*). There is reciprocal movement of the proximal carpal row in the ulnar direction (*white arrow*). The proximal carpal row flexes and the distal scaphoid pole may assume a signet-ring appearance (*arrowheads*). Note the decreased apposition of the lunate (*L*) with the distal radial articular surface. **b** With ulnar deviation the reverse occurs. The distal carpal row and metacarpal bones move in the ulnar direction (*black arrow*), whereas the proximal carpal row moves radially (*white arrow*). Observe the increased apposition of the lunate (*L*) with the distal radial articular surface. There is unified extension of the proximal carpal row, with the scaphoid assuming an elongated appearance

dynamic SL instability [28]. Rotatory subluxation of the scaphoid may manifest on the lateral flexion view.

Complete tear of the SL ligament, along with primary or secondary injuries to the secondary stabilizing ligaments, results in static SL instability [37, 38]. Classic signs of SL dissociation are evident on routine wrist radiographs. The scaphoid and lunate, free from the constraints of an intact SL ligament, rotate in opposite directions. There is flexion of the distal pole of the scaphoid (rotatory subluxation of the scaphoid or stage I of the Mayfield classification of progressive perilunar instability; Fig. 7) [41]. On the lateral radiograph, the flexed scaphoid may ride on the dorsal rim of the radius, whereas on the PA radiograph it may demonstrate a foreshortened appearance with the so-called "signet-ring" sign (Fig. 7). An SL angle of greater than 70° is considered highly suggestive of rotatory subluxation of the scaphoid [6]. Disruption of Gilula's arcs I/II, along with diastasis of the SL interval (Terry Thomas sign) may also be evident on PA radiographs [7].

With further damage, a DISI deformity develops, with dorsal tilting/extension of the lunate, and dorsal and proximal translation of the capitate and distal carpal row [5]. The tilted lunate may assume a triangular morphology (instead of its normal trapezoidal shape) on PA radiographs. The scaphoid may flex and along with the extended lunate results in an increased SL angle on lateral radiographs (an SL angle ≥80° is considered abnormal, and an SL angle of 60°–80° is questionably abnormal; Fig. 8) [22]. The postural changes in DISI

Fig. 7 A 30-year-old man with rotatory subluxation of the scaphoid. **a** PA wrist radiograph demonstrates widening of the SL interval: The SL interval measures 5 mm and is disproportionately widened relative to other intercarpal joints. The scaphoid has a foreshortened appearance and its flexed distal pole is seen end-on, producing the "signet-ring" sign (*arrowheads*). **b** Lateral wrist radiograph shows flexion of the distal scaphoid pole (*arrowheads*) with increased SL angle (not shown; SL angle measures 89°). The capitolunate angle measures 21° (not shown) and is within normal limits

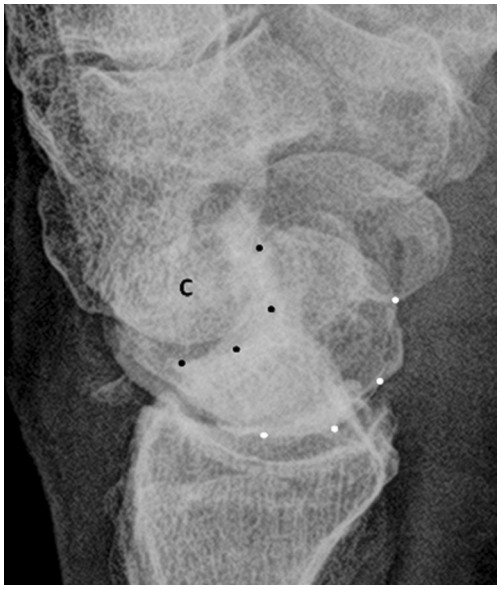

Fig. 8 A 55-year-old man with dorsal intercalated segmental instability (DISI). Lateral wrist radiograph shows the extended lunate with its distal concave articular surface (*black dots*) facing dorsally. There is also volar displacement of the lunate at the radiocarpal joint, with its proximal convex articular surface (*white dots*) overriding the palmar rim of the distal radius. The capitate (*C*) moves proximally and dorsally in conjunction with the extended lunate. The SL angle (not shown) is increased and measures 110°

are reversible initially, and become progressively irreversible as the result of secondary changes (including capsular contracture) in the surrounding supporting ligaments [6].

Fig. 9 A 40-year-old woman with SL advanced collapse (SLAC III). PA wrist radiograph shows osteoarthritis of the radioscaphoid (*black arrows*) and capitolunate (*white arrow*) joints, with proximal migration of the capitate and decreased carpal height (*black line*). There is widening of the SL interval (6 mm). Observe the calcific deposits (*arrowheads*) along the radial aspect of the scaphoid and in the triangular fibrocartilage and lunotriquetral joint

Fig. 10 A 45-year-old man with scaphoid nonunion advanced collapse (SNAC I). The PA wrist radiograph demonstrates a nonunion scaphoid wrist fracture (*black arrows*) with a fragmented proximal scaphoid pole (*dots*). There is severe degenerative narrowing of the scaphoid–radial styloid interspace (*white arrows*)

In the final stage there is progressive degeneration and collapse of the carpus, known as SL advanced collapse (SLAC). Initially, osteoarthritis is limited to the radial styloid–scaphoid portion of the radioscaphoid joint (SLAC I),

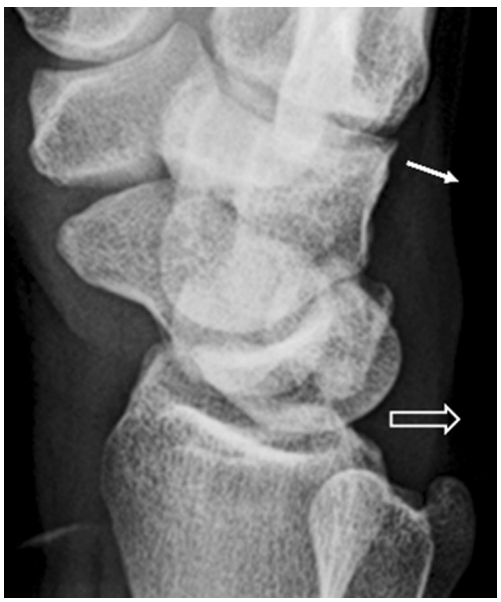

Fig. 11 A 30-year-old woman with volar intercalated segmental instability (VISI). A lateral wrist radiograph shows a flexed lunate with its distal concave articular surface rotated volarly. The lunate has moved dorsally (*thick arrow*) and its proximal convex articular surface is seen overriding the dorsal rim of the distal radius. The capitate head moves with the flexed lunate in a proximal and volar direction, whereas its distal pole tilts dorsally (*thin arrow*). Overall, the lunate and capitate orientations produce a zigzag deformity. The SL angle (not shown) is decreased measuring 12° and the capitolunate angle (not shown) is increased measuring 45°

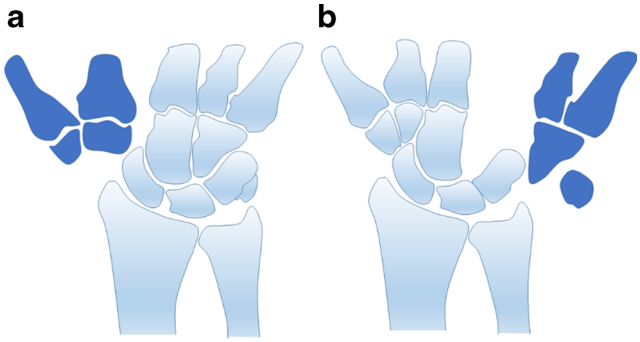

Fig. 12 Axial radial and ulnar dislocations. **a** Peritrapezoid peritrapezium axial radial dislocation. With axial radial dislocation, the distal carpus splits longitudinally into two columns: the ulnar column (*light blue*) is stable with regard to the radius, and the radial column (*dark blue*) displaces most commonly in the radial and proximal direction. **b** Perihamate peripisiform axial ulnar dislocation. In ulnar disruptions, the radial column (*light blue*) is stable with regard to the radius, and the ulnar column (*dark blue*) displaces most commonly in the ulnar and proximal direction. Axial disruptions may be purely ligamentous (as illustrated) or associated with fractures of the carpal bones

progressing to involve the entire radioscaphoid joint (SLAC II), the scaphocapitate and/or capitolunate joints (SLAC III; Fig. 9), and eventually the whole carpus (SLAC IV) [42–44]. Carpal instability arising from a nonunion scaphoid fracture can progress through relatively comparable degenerative stages, to pancarpal arthrosis, and is known as "scaphoid nonunion advanced collapse" (SNAC; Fig. 10) [43].

Fig. 13 A 10-year-old girl with transtrapezium, peritrapezoid axial radial fracture dislocation. PA wrist radiograph demonstrates a sagittal plane fracture of the trapezium (fracture fragments are demarcated by *white arrows*). The first metacarpal and the radial portion of the fractured trapezium are dislocated proximally and radially. The peritrapezoid portion of the injury is seen as subtle widening between the second and third metacarpal bases (*arrowhead*) and diastasis of the trapezoid–capitate interval (*black arrow*). There is proximal displacement of the second, relative to the third metacarpal base. There is extensive soft-tissue injury at the first web interspace

Table 1 Classification of perilunate injuries according to Mayfield et al. [41]

Classification	Joints disrupted
Stage I (SL dissociation or rotatory subluxation of the scaphoid)	Scapholunate
Stage II (perilunate dislocation)	Scapholunate, capitolunate
Stage III (midcarpal dislocation)	Scapholunate, capitolunate, triquetrolunate
Stage IV (lunate dislocation)	Scapholunate, capitolunate, triquetrolunate, radiolunate

Radiographic measurements for carpal collapse in SLAC

Carpal height can be used to quantify carpal collapse and determine disease progression on serial radiographs. On a PA radiograph, carpal height is the distance between the third metacarpal base and the distal radial articular surface, as measured along a line coursing through the central long axis of the third metacarpal (Fig. 9). The carpal height ratio is the carpal height divided by the third metacarpal length, with normal values of 0.54 ± 0.03 (mean ± standard deviation) [45]. The carpal height index is obtained by dividing the carpal height ratio of the diseased wrist by that of the normal wrist, with normal values of 1.000 ± 0.015 [45]. None of these three measurements allows comparison among individuals [17].

Proximal row CID: lunotriquetral instability

Lunotriquetral (LT) instability usually results from injury to the LT ligament [8, 46]. The mechanism of injury is variable and includes attrition by age, positive ulnar variance, and perilunate (or reverse perilunate) injuries [8, 41]. History of a specific injury (such as a fall on the outstretched hand) is usually recalled. With LT instability, the carpus may collapse in a VISI configuration.

The radiographic appearance of wrists with LT ligament tears is often normal [8]. When static LT dissociation is present, PA radiographs demonstrate disruption of Gilula's arcs, along with proximal migration of the triquetrum and/or LT overlap [24, 47]. It must be emphasized that in contrast to SL dissociation, LT diastasis is rarely observed on PA radiographs [26]. With VISI configuration, the lunate may demonstrate a triangular shape on the PA view. On the lateral view,

Fig. 14 A 25-year-old man with dorsal perilunate dislocation. **a** PA wrist radiograph: the lunate maintains its trapezoidal shape and parallel relationship with the distal radius, ruling out a lunate dislocation. There is disruption of Gilula's arcs I–III, overlap of the SL and capitolunate articular surfaces and step-off of the lunotriquetral joint. Findings are suggestive of perilunate dislocation. **b** Lateral wrist radiograph: the lunate is centered normally over the distal radius, and the rest of the carpal bones (localized by the capitate) are dislocated dorsally

the lunate is flexed, the capitate is translated volarly (whereas its distal pole may be tilted dorsally), the triquetrum is extended, and there is an increased capitolunate angle and/or decreased SL angle (Fig. 11) [24]. Stress views or fluoroscopy with dynamic motion studies are necessary to elucidate abnormalities with dynamic LT instability [7, 10, 46].

Distal carpal row CID: axial instability

Axial dissociation of the carpus is a traumatic longitudinal disruption of the radial and ulnar-sided bones of the distal carpal row from each other [48–50]. The distal carpal row has a high degree of intrinsic biomechanical stability [51]. Therefore, distal carpal row dissociations are rare, typically result from blast or crush injuries, and are usually associated with extensive soft-tissue injuries [50, 52].

Axial dissociations may occur on the radial or ulnar side of the wrist and may be classified into three groups: axial ulnar disruption, axial radial disruption, and combined disruptions (Figs. 12, 13) [48]. Distal carpal row disruptions may be purely ligamentous or associated with fractures of the carpal bones. In the nomenclature for these dissociations, the prefix "peri" indicates that the dislocation is around a bone, and "trans" denotes that the dislocation is associated with a fracture through that bone.

It must be stressed that axial instability does not always imply gross carpal injuries. Meticulous attention to subtle

Fig. 15 A 30-year-old man with transulnar styloid volar lunate fracture–dislocation. **a** PA wrist radiograph shows an empty lunate bed with the dislocated lunate (*black arrows*) projecting over the distal radius. There is an ulnar styloid base fracture (*white arrow*). The rest of the carpal bones demonstrate normal alignment (the capitohamate joint is not profiled on this image). **b** Lateral wrist radiograph: the dislocated lunate is displaced volarly and rotated 180° in the clockwise direction (*curved arrow*). The capitate head (*dots*) is centered over the distal radius and the *arrowhead* shows the avulsed ulnar styloid fragment

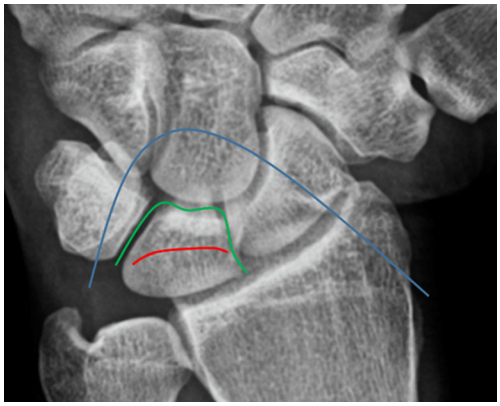

Fig. 16 Arcs of injury in perilunate injuries. PA wrist radiograph: greater arc of injury (*blue*), lesser arc of injury (*green*), and translunate arc of injury (*red*)

malalignment of the carpus is necessary so that this diagnosis is not overlooked in subtle cases [50, 53].

Carpal instability nondissociative: midcarpal instability

Midcarpal instability is a controversial entity with poorly understood etiology and pathomechanics [3, 53]. It appears to represent distinct clinical entities that result from abnormal kinematics at the midcarpal and sometimes the radiocarpal joints [2, 54]. The discussion of midcarpal instability is beyond the scope of this article. Of note, plain radiography is not typically helpful for diagnosis. Nondissociative radiocarpal instability will be discussed subsequently with "adaptive carpus" (see section "Radiocarpal instability (carpal instability nondissociative); adaptive carpus" below).

Fig. 17 A 45-year-old woman with rheumatoid arthritis and ulnar translocation (Taleisnik type I) of the carpus. PA wrist radiograph shows ulnar translocation of the carpus with decreased radiolunate apposition and widening (3.5 mm) of the scaphoid–radial styloid interspace (*white line*)

Fig. 18 A 24-year-old woman with Madelung's deformity. PA wrist radiograph shows increased radial inclination (measuring 39°; see Fig. 19) secondary to shortening of the ulnar aspect of the distal radius. The proximal carpal row "adapts" to the deformed distal radius: there is proximal migration of the lunate with resultant V-shaped configuration of the proximal carpal row

Carpal instability complex/perilunate injuries

Complex carpal instability includes combined dissociative and nondissociative injuries. Most of these instabilities are secondary to perilunate injuries [3], which result from high-energy loads that lead to ligamentous and/or osseous disruptions [55]. Mayfield et al. [41] observed that progressive loads on cadaveric wrists positioned in hyperextension, ulnar deviation, and intercarpal supination can produce reproducible patterns of perilunate injuries (Table 1) that progress from a radial to an ulnar direction. Stage I involves SL ligament disruption (SL dissociation or rotatory subluxation of the scaphoid). At stage II, there is disruption of the capitolunate articulation, with the capitate dislocating most commonly dorsally (Fig. 14). Lunotriquetral ligament disruption occurs at stage III. At stage IV, the lunate dislocates from its fossa, and the capitate becomes aligned with the radius (Fig. 15). Stage I is categorized as dissociative carpal instability, whereas stages II to IV are considered complex carpal instabilities.

The Mayfield classification describes "lesser arc injuries" with only ligamentous disruptions accounting for the perilunate injuries (Fig. 16) [56]. When there is/are superimposed fracture/s of the bones surrounding the lunate, the injury is referred to a "greater arc injury" or a perilunate fracture dislocation (Fig. 16) [56]. The nomenclature of perilunate fracture dislocations uses the "trans" prefix to denote the fractured bone. The scaphoid and radial styloid are the most commonly fractured bones in perilunate fracture dislocations. More recently, the concept of lesser and greater arc

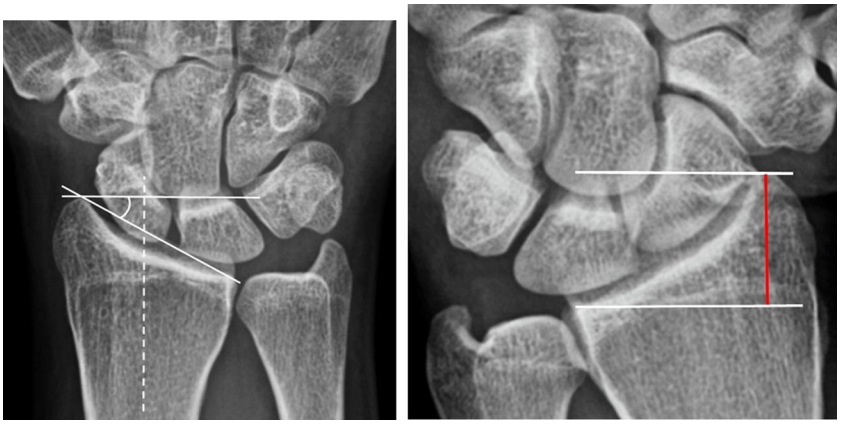

Fig. 19 Distal radial measurements on normal PA wrist radiographs. **a** Radial inclination is the angle formed between a line connecting the radial styloid tip to the ulnar aspect of the distal radius, and a line perpendicular to the longitudinal axis of the distal radius (normal values = 16°–28°). **b** Radial length (*red line*) is the distance between two parallel lines perpendicular to the longitudinal axis of the distal radius, with one line coursing along the distal radial styloid tip, and the other line coursing along the distal surface of the sigmoid notch (average radial length measures 10–13 mm)

injuries has been expanded to include a "translunate arc" where the fracture courses through the lunate (Fig. 16) [57].

Herzberg et al. [58] classified perilunate injuries into perilunate dislocations or fracture–dislocations (stage I) and lunate dislocations (stage II). Mayfield's stages I to III are considered to equate to stage I injuries in the Herzberg classification, whereas Mayfield's stage IV corresponds to stage II in the Herzberg classification.

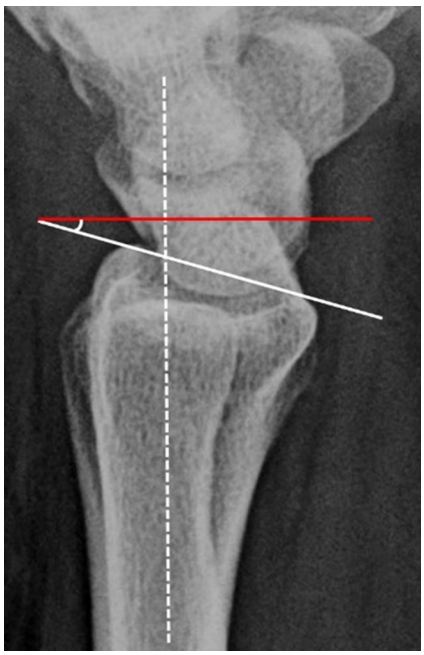

Fig. 20 Palmar tilt measurement on a normal lateral wrist radiograph. The palmar tilt is the angle subtended between a line connecting the distal-most points of the radius (*white line*), and a line perpendicular (*red line*) to the long axis of the radius (*dashed line*). The normal palmar tilt averages 11° and has a range of 2°–20°. Negative values for palmar tilt are not normal

Radiocarpal instability (carpal instability nondissociative); adaptive carpus

Translocation of the entire carpus can occur at the level of the radiocarpal joint in the ulnar, volar, dorsal or rarely radial directions. The cause of these translocations may be either injury of the extrinsic carpal ligaments, or carpal malpositioning secondary to distal radius/ulnar anatomical abnormalities. The former is considered to be largely a subcategory of "carpal instability nondissociative," whereas the latter is classified as "adaptive" carpus [3].

Under physiological conditions, the extrinsic carpal ligaments resist the tendency of the carpus to slide down the ulnar and palmar tilts of the distal radius. Injury of these ligaments (such as may occur with trauma, rheumatoid arthritis or calcium pyrophosphate deposition disease) may predispose to radiocarpal instability and ulnar translocation of the carpus [10, 32]. Two different patterns of ulnar translocation have been described [59]. The entire carpus may migrate in the ulnar direction along the normal slope of the distal radius (Taleisnik type I; Fig. 17). There is a resultant widening (more than 2 mm) of the scaphoid–radial styloid interspace and decreased (<50 %) radiolunate apposition [40]. With intact radial extrinsic ligaments, the scaphoid remains in place, whereas the lunate–triquetrum translocates in the ulnar direction, causing an SL diastasis (Taleisnik type II). This latter type of ulnar translocation is considered a "carpal instability complex" subcategory. Ulnar translocation predisposes to radiocarpal osteoarthritis [59].

Adaptive radiocarpal instability may be seen with malunited distal radial fractures, Madelung's deformity (Fig. 18), or excessive resection of the radial styloid process or ulnar head [5, 60, 61].

Radiographic assessments in radiocarpal instability and adaptive carpus

Assessment for ulnar translocation is performed on PA radiographs. In a normal wrist, one half or more of the lunate should oppose the distal radial articular surface. Three radiographic measurements are commonly used for evaluation of the distal radius: radial inclination, radial length, and palmar tilt (Figs. 19, 20) [17, 62, 63].

Conclusion

Various and at times complex patterns of carpal instability can occur. Familiarity with the most commonly used concepts of carpal instability classification is important for the correct interpretation of images. PA and lateral wrist radiographs are the first line of imaging in carpal instability. Additional information may be obtained with the use of stress radiographs and other imaging modalities.

Compliance with ethical standards

Conflicts of interest The authors indicate that they have no conflicts of interest.

Financial disclosures None.

References

1. Linscheid RL, Dobyns JH. Dynamic carpal stability. Keio J Med. 2002;51:140–7.
2. Wolfe SW, Garcia-Elias M, Kitay A. Carpal instability nondissociative. J Am Acad Orthop Surg. 2012;20:575–85.
3. Carlsen BT, Shin AY. Wrist instability. Scand J Surg. 2008;97:324–32.
4. May O. The pisiform bone: sesamoid or carpal bone? Ann Chir Main Memb Super. 1996;15:265–71.
5. Linscheid RL, Dobyns JH, Beabout JW, Bryan RS. Traumatic instability of the wrist. Diagnosis, classification, and pathomechanics. J Bone Joint Surg Am. 1972;54:1612–32.
6. Kitay A, Wolfe SW. Scapholunate instability: current concepts in diagnosis and management. J Hand Surg Am. 2012;37:2175–96.
7. Loredo RA, Sorge DG, Garcia G. Radiographic evaluation of the wrist: a vanishing art. Semin Roentgenol. 2005;40:248–9.
8. Shin AY, Battaglia MJ, Bishop AT. Lunotriquetral instability: diagnosis and treatment. J Am Acad Orthop Surg. 2000;8:170–9.
9. Taleisnik J. The ligaments of the wrist. J Hand Surg. 1976;1A:110–8.
10. Schmitt R, Froehner S, Coblenz G, Christopoulos G. Carpal instability. Eur Radiol. 2006;16:2161–78.
11. Theumann NH, Etechami G, Duvoisin B, Wintermark M, Schnyder P, Favarger N, et al. Association between extrinsic and intrinsic carpal ligament injuries at MR arthrography and carpal instability at radiography: initial observations. Radiology. 2006;238:950–7.
12. Short WH, Werner FW, Green JK, Masaoka S. Biomechanical evaluation of the ligamentous stabilizers of the scaphoid and lunate: part II. J Hand Surg Am. 2005;30:24–34.
13. Short WH, Werner FW, Green JK, Sutton LG, Brutus JP. Biomechanical evaluation of the ligamentous stabilizers of the scaphoid and lunate: part III. J Hand Surg Am. 2007;32:297–309.
14. Ruby LK, Cooney III WP, An KN, Linscheid RL, Chao EY. Relative motion of selected carpal bones: a kinematic analysis of the normal wrist. J Hand Surg Am. 1988;13:1–10.
15. Kauer JM. The interdependence of carpal articulation chains. Acta Anat (Basel). 1974;88:481–501.
16. Horii E, Garcia-Elias M, An KN, Bishop AT, Cooney WP, Linscheid RL, et al. A kinematic study of luno-triquetral dissociations. J Hand Surg Am. 1991;16:355–62.
17. Mann FA, Wilson AJ, Gilula LA. Radiographic evaluation of the wrist: what does the hand surgeon want to know? Radiology. 1992;184:15–24.
18. Jedlinski A, Kauer JMG, Jonsson K. X-ray evaluation of the true neutral position of the wrist: the groove for extensor carpi ulnaris as a landmark. J Hand Surg Am. 1995;20:511–2.
19. Levis CM, Yang Z, Gilula LA. Validation of the extensor carpi ulnaris groove as a predictor for the recognition of standard posteroanterior radiographs of the wrist. J Hand Surg Am. 2002;27(2):252–7.
20. Schmitt R, Lanz U. Diagnostic imaging of the hand. 1st ed. Stuttgart: Thieme; 2007. p. 4–5.
21. Yang Z, Mann FA, Gilula LA, Haerr C, Larsen F. Scaphopisocapitate alignment: criterion to establish a neutral lateral view of the wrist. Radiology. 1997;205:865–9.
22. Gilula LA. Carpal injuries: analytic approach and case exercises. AJR Am J Roentgenol. 1979;133:503–17.
23. Viegas SF, Wagner K, Patterson R, Peterson P. Medial (hamate) facet of the lunate. J Hand Surg Am. 1990;15A:564–71.
24. Gilula LA, Weeks PM. Post-traumatic ligamentous instabilities of the wrist. Radiology. 1978;129:641–51.
25. Sarrafian SK, Melamed JL, Goshgarian GM. Study of wrist motion in flexion and extension. Clin Orthop Relat Res. 1977;126:153–9.
26. Schmitt R, Lanz U. Diagnostic imaging of the hand. 1st ed. Stuttgart: Thieme; 2007. p. 269–92.
27. Truong NP, Mann FA, Gilula LA, Kang SW. Wrist instability series: increased yield with clinical-radiologic screening criteria. Radiology. 1994;192:481–4.
28. Lee SK, Desai H, Silver B, Dhaliwal G, Paksima N. Comparison of radiographic stress views for scapholunate dynamic instability in a cadaver model. J Hand Surg Am. 2011;36:1149–57.
29. Lawand A, Foulkes GD. The "clenched pencil" view: a modified clenched fist scapholunate stress view. J Hand Surg Am. 2003;28:414–20.
30. Gilula LA, Yin Y. Imaging of the wrist and hand. Philadelphia: Saunders; 1996. p. 373–84.
31. Cooney WP, Linscheid RL, Dobyns JH. The wrist: diagnosis and operative treatment. St. Louis: Mosby; 1998. p. 490–500.
32. Resnick D, Niwayama G. Carpal instability in rheumatoid arthritis and calcium pyrophosphate deposition disease. Ann Rheum Dis. 1977;36:311–8.
33. Schmitt R, Heinze A, Fellner F, Obletter N, Strühn R, Bautz W. Imaging and staging of avascular osteonecroses at the wrist and hand. Eur J Radiol. 1997;25:92–103.
34. Drewniany JJ, Palmer AK, Flatt AE. The scaphotrapezial ligament complex: an anatomic and biomechanical study. J Hand Surg Am. 1985;10:492–8.

35. Watson HK, Ashmead IV D, Makhlouf MV. Examination of the scaphoid. J Hand Surg Am. 1988;13:657–60.
36. Nathan R, Blatt G. Rotary subluxation of the scaphoid. Revisited. Hand Clin. 2000;16:417–31.
37. Taleisnik J. Classification of carpal instability. Bull Hosp Jt Dis Orthop Inst. 1984;44:511–31.
38. Short WH, Werner FW, Green JK, Masaoka S. Biomechanical evaluation of ligamentous stabilizers of the scaphoid and lunate. J Hand Surg Am. 2002;27:991–1002.
39. Ruby LK, An KN, Linscheid RL, Cooney 3rd WP, Chao EY. The effect of scapholunate ligament section on scapholunate motion. J Hand Surg Am. 1987;12:767–71.
40. Linn MR, Mann FA, Gilula LA. Imaging the symptomatic wrist. Orthop Clin North Am. 1990;21:515–43.
41. Mayfield JK, Johnson RP, Kilcoyne RK. Carpal dislocations: pathomechanics and progressive perilunar instability. J Hand Surg Am. 1980;5:226–41.
42. Watson HK, Ballet FL. The SLAC wrist: scapholunate advanced collapse pattern of degenerative arthritis. J Hand Surg Am. 1984;9A:358–65.
43. Watson H, Ryu J. Evolution of arthritis of the wrist. Clin Orthop Relat Res. 1986;202:57–67.
44. Weiss KE, Rodner CM. Osteoarthritis of the wrist. J Hand Surg Am. 2007;32:725–46.
45. Stahelin A, Pfeiffer K, Sennwald G, Segmuller G. Determining carpal collapse: an improved method. J Bone Joint Surg Am. 1989;71:1400–5.
46. Viegas SF, Patterson RM, Peterson PD, Pogue DJ, Jenkins DK, Sweo TD, et al. Ulnar-sided perilunate instability: an anatomic and biomechanic study. J Hand Surg Am. 1990;15:268–78.
47. Reagan DS, Linscheid RL, Dobyns JH. Lunotriquetral sprains. J Hand Surg Am. 1984;9:502–14.
48. Garcia-Elias M, Dobyns JH, Cooney III WP, Linscheid RL. Traumatic axial dislocations of the carpus. J Hand Surg Am. 1989;14:446–57.
49. Cooney WP, Bussey R, Dobyns JH, Linscheid RL. Difficult wrist fractures. Perilunate fracture-dislocations of the wrist. Clin Orthop Relat Res. 1987;214:136–47.
50. Weiss AC, Berger RA. Hand surgery. Philadelphia: Lippincott Williams and Wilkins; 2004. p. 534–47.
51. Garcia-Elias M, An KN, Cooney WP, Linscheid RL, Chao EY. Transverse stability of the carpus. J Orthop Res. 1989;7:738–43.
52. Shin AY, Glowacki KA, Bishop AT. Dynamic axial carpal instability: a case report. J Hand Surg Am. 1999;24:781–5.
53. Reinsmith LE, Garcia-Elias M, Gilula LA. Traumatic axial dislocation injuries of the wrist. Radiology. 2013;267:680–9.
54. Lichtman DM, Wroten ES. Understanding midcarpal instability. J Hand Surg Am. 2006;31:491–8.
55. Sawardeker PJ, Kindt KE, Baratz ME. Fracture-dislocations of the carpus: perilunate injury. Orthop Clin North Am. 2013;44:93–106.
56. Johnson RP. The acutely injured wrist and its residuals. Clin Orthop Relat Res. 1980;149:33–44.
57. Bain GI, McLean JM, Turner PC, Sood A, Pourgiezis N. Translunate fracture with associated perilunate injury: 3 case reports with introduction of the translunate arc concept. J Hand Surg Am. 2008;33:1770–6.
58. Herzberg G, Comtet JJ, Linscheid RL, Amadio PC, Cooney WP, Stalder J. Perilunate dislocations and fracture-dislocations: a multicenter study. J Hand Surg Am. 1993;18:768–79.
59. Taleisnik J. Current concepts review. Carpal instability. J Bone Joint Surg Am. 1988;70:1262–8.
60. Dumontier C, Meyer ZU, Reckendorf G, Sautel A, Lenoble E, Saffar P, et al. Radiocarpal dislocations: classification and proposal for treatment: a review of twenty-seven cases. J Bone Joint Surg Am. 2001;83A:212–8.
61. Moneim MS, Bolger JT, Omer GE. Radiocarpal dislocation—classification and rationale for management. Clin Orthop. 1985;192:199–209.
62. Goldfarb CA, Yin Y, Gilula LA, Fisher AJ, Boyer MI. Wrist fractures: what the clinician wants to know. Radiology. 2001;219:11–28.
63. Altissimi M, Antenucci R, Fiacca C, Mancini GB. Long-term results of conservative treatment of fractures of the distal radius. Clin Orthop Relat Res. 1986;206:202–10.